Clays and Clay Minerals, Vol. 55, No. 4, 339–347, 2007.

ON THE KINETICS OF ION EXCHANGE IN PHLOGOPITE – AN *IN SITU* AFM STUDY

KIRILL ALDUSHIN[1], GUNTRAM JORDAN[1,*], ELENA ALDUSHINA[2] AND WOLFGANG W. SCHMAHL[1]

[1] Department für Geo- und Umweltwissenschaften, Sektion Kristallographie, Ludwig-Maximilians-Universität, Theresienstraße 41, 80333 München, Germany

[2] Institut für Geologie, Mineralogie und Geophysik, Ruhr-Universität Bochum, 44780 Bochum, Germany

Abstract—The kinetics of cation exchange in phlogopite have been studied *in situ* by hydrothermal atomic force microscopy (HAFM). The exchange of interlayer K by octylammonium ions caused an increase in the interlayer distance and the formation of reaction fronts which can be locally resolved by AFM. The observed reaction fronts revealed substantial variations in their propagation rates – even within single interlayers. This observed variability in interlayer reactivity could mainly be attributed to chemical and structural inhomogeneities of the samples. A quantitative evaluation of the front propagation at representative sites yielded a diffusion coefficient of the K^+ exchange by octylammonium of $1.2\pm0.6\times10^{-11}$ cm^2/s assuming negligible transport normal to the layers. The reverse reaction, *i.e*. the exchange of organic ions by K^+, resulted in a retreat of the reaction fronts and a general restoration of the original morphological state. However, indications of structural alterations and areas with trapped octylammonium ions were found.

Key Words—Alkylammonium, Atomic Force Microscopy, Clays, Cation Exchange, Diffusion, Mica, Organic Ions, Phyllosilicates, Surface Alteration, Swelling.

INTRODUCTION

Ion exchange in phyllosilicates is one of the most extensively studied topics in clay mineralogy. This interest stems from the importance of ion exchange in fundamental geochemistry, chemical engineering, water-treatment technology, and in technical applications. Ion-exchange reactions are also used to characterize or identify specific minerals among the 2:1 phyllosilicates (*e.g*. Lagaly, 1981). One characterization technique is based on the exchange reaction between the interlayer cations and n-alkylammonium ions from the solution (*e.g*. Lagaly and Weiss, 1969; Laird *et al.*, 1987; Mermut and Lagaly, 2001). This alkylammonium exchange method can be used to measure the layer charge because the arrangement and tilt angle of alkylammonium ions within the interlayer depend primarily on the layer-charge density. In micas this angle is close to 90º, *i.e*. the alkylammonium chains are oriented almost perpendicular to the phyllosilicate layers (Weiss, 1963; Ghabru *et al*., 1989; Marcks *et al.*, 1989). The kinetics of the K^+-alkylammonium exchange reaction and the resulting changes in interlayer distances depend on experimental parameters and on the chemical composition of the samples. Many studies report on difficulties in reproducing the reactivity of sheet silicates with organic substances. For example, Vali *et al*. (1992) studied the K^+-alkylammonium exchange in phlogopite and vermiculite by using high-resolution transmission electron microscopy (HRTEM). These authors showed that some of the layers did not react with alkylammonium and that the samples occasionally exhibit alternating layers of alkylammonium and K^+. The authors concluded that this behavior is due to chemical variations of the sample. Ferrow *et al*. (1999) studied the reaction products of biotite with dodecylammonium by HRTEM. They showed that the replacement of the interlayer K^+ by organic ions is quasi-periodic and does not affect all available interlayers simultaneously. The authors further proposed a double-layer arrangement of the dodecylammonium ions oriented normal to the silicate layers. Structural and chemical peculiarities of the samples also affect the ion exchange in mica-inorganic systems. Kodama and Ross (1973) studied the rate of K^+ exchange by Ca^{2+} in phlogopites with a constant layer charge but different tetrahedral and octahedral ionic substitution. They concluded that mica layers are more expandable when their charge is located in the octahedral sheet. Barshad and Kishk (1968) showed that oxidation of octahedral Fe in vermiculites and biotites increases the K^+-fixation capacity of vermiculite and increases the difficulty in replacing interlayer K^+ by inorganic cations in biotites.

In spite of a great number of X-ray diffraction (XRD) and HRTEM studies concerning the ion exchange in phyllosilicates, just a few studies have explored the kinetics of the process. Mackintosh *et al*. (1971) investigated the exchange of K^+ by dodecylammonium in micas. Based on measurements of the amount of K^+ released into the solution, the authors concluded that the reaction is controlled by diffusion until ~50% of K^+ is substituted by alkylammonium ions. Newman (1970) investigated the synergetic effect of protons on the exchange of K^+ by Na^+ in different micas and concluded

* E-mail address of corresponding author:
guntram.jordan@lrz.uni-muenchen.de
DOI: 10.1346/CCMN.2007.0550401

that the results obtained cannot be explained by a simple diffusion process. Rausell-Colom *et al*. (1964) measured the movement of ion-exchange fronts in micas by optical microscopy. The fronts emanated from the crystal edges and consisted of $2-5\times10^6$ layers. The measurements revealed a linear dependence between the distance passed by the fronts and the square root of time. Rausell-Colom *et al*. (1964) concluded that the rate of K^+ substitution by Sr^{2+} and other inorganic cations is controlled by diffusion.

Atomic force microscopy provides an *in situ* access to solid-liquid interfaces with high resolution and therefore can help to unravel the kinetics of the ion-exchange reactions of phyllosilicates. Furthermore, by using HAFM, information about the alteration kinetics of phyllosilicates at elevated temperatures can be obtained (*e.g*. Aldushin *et al*., 2006). In the present study, HAFM was used to investigate the kinetics of the K^+-octylammonium exchange reaction in different phlogopite crystals.

EXPERIMENTAL

Natural phlogopite crystals from three different locations (No. 1: Särkilampi, Finland; No. 2. Tranomaro, Madagascar; and No. 3: Andranodambo, Madagascar) were used for electron microprobe analysis (EMPA): see Table 1. For AFM experiments, the crystals were cleaved immediately before affixing them within the fluid cell underneath a titanium wire which runs across the sample mount. The samples were 0.1−0.4 mm thick with a (001) surface area of ~15−25 mm^2. After the fluid cell (volume $\approx$0.5 mL) had been filled with solution, the cell was closed. For hydrothermal experiments the cell was subsequently pressurized, and heated to the temperature of interest ($\leqslant$80ºC). The experiments ran for up to 60 h at room temperature and up to 15 h at elevated temperatures. Solution flow rates through the fluid cell were set from 0 to 10 µL/s. All *in situ* measurements were carried out using a contact-mode hydrothermal atomic force microscope which was constructed in our laboratories (Higgins *et al*., 1998; Jordan *et al*., 2001). All AFM images are presented in deflection mode (appear as illuminated from the left). Uncoated Si cantilevers with integrated tips (spring constant: 0.1−0.3 N/m) were used. Loading forces were kept below 10 nN unless stated otherwise. The surfaces were routinely checked for potential scan-induced effects by scan-size variations.

In this study, 0.5 M octylammonium chloride ($(CH_3(CH2)_7NH_3^+Cl^-)$) and 0.5 M potassium chloride solutions were used. According to Ruehlicke and Kohler (1981), the 0.5 M concentration of octylammonium ions is optimal for the exchange reaction. The octylammonium chloride solution was prepared according to the procedure described by Lagaly (1991); the pH value of the solution was adjusted to 7 at room temperature by adding HCl. Reagent-grade chemicals and high-purity deionized water (resistivity: 18 MΩ cm) were used. Control experiments (without added octylammonium ions) were performed using deionized water exclusively.

RESULTS

K^+ → *octylammonium*

Figure 1a shows three cleavage steps (heights: 3, 1 and 11 nm − from left to right) on an unreacted basal surface of phlogopite No. 1 at room temperature. Figure 1b shows the formation of swelling fronts at these cleavage steps. The fronts can be attributed to an ion-exchange reaction between the interlayer K^+ and octylammonium ions. The reaction fronts emerged at all three steps almost simultaneously, but propagation of the swelling fronts was not always uniform (fast propagating front parts are marked with white arrows). At all three steps, the layers expanded by ~18 Å. At the right cleavage step a second front (Figure 1c, white arrow 2) began to propagate (nucleation of the front is marked with a black arrow in Figure 1b). This second front intersected with the first front (white arrow 1) but did not interact. Therefore it is suggested that the two fronts represented ion-exchange reactions in different inter-

Table 1. EMPA of the phlogopite samples (compound, wt.%).

	Phlogopite 1		Phlogopite 2		Phlogopite 3	
	mean	std. dev.	mean	std. dev.	mean	std. dev.
SiO_2	40.879	1.388	38.520	0.173	40.842	0.138
Al_2O_3	10.298	0.366	16.109	0.074	13.756	0.083
K_2O	9.615	1.509	10.304	0.055	10.665	0.147
MgO	23.005	0.520	22.839	0.156	24.957	0.077
FeO	8.622	2.058	4.487	0.057	2.696	0.013
TiO_2	0.342	0.058	1.089	0.408	0.565	0.032
Na_2O	0.042	0.018	0.304	0.021	0.190	0.016
F	0.927	0.042	1.667	0.034	6.683	0.028
Total	93.73		95.01		100.354	

std. dev. − standard deviation

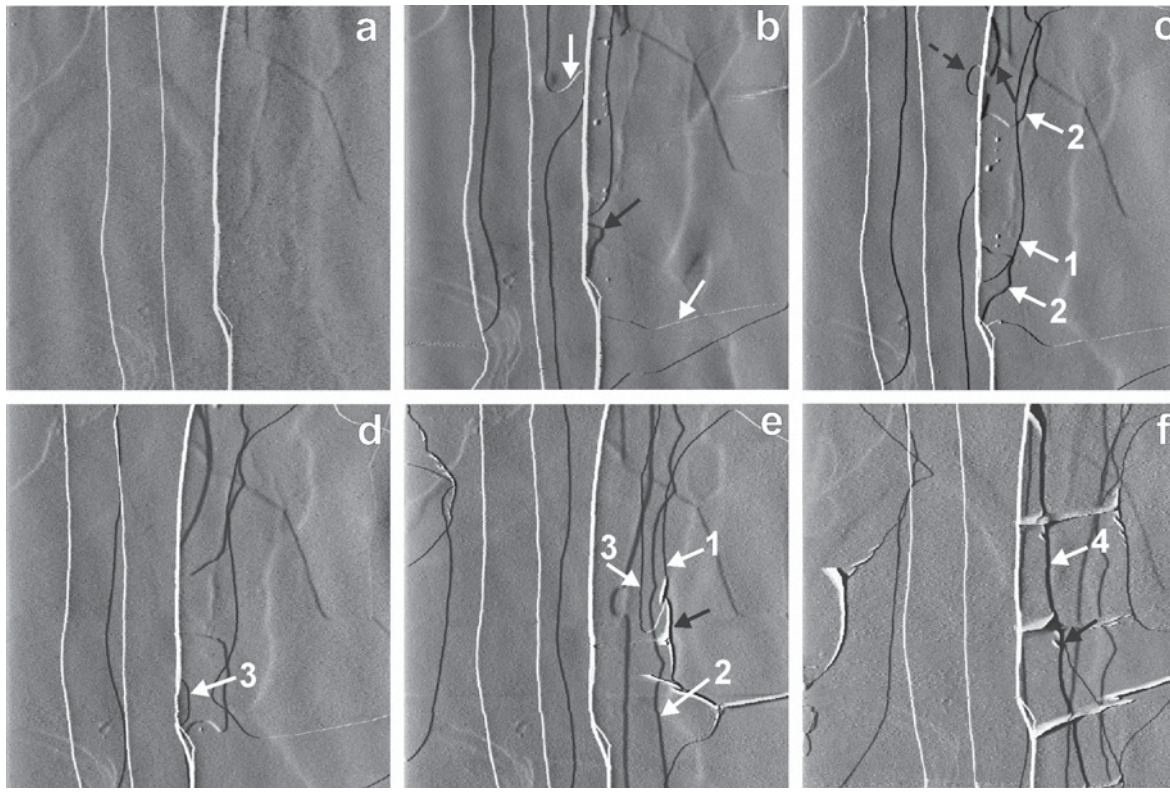

Figure 1. Ion-exchange reaction $K^+ \rightarrow$ octylammonium at 20ºC: (a) pristine phlogopite surface with cleavage steps; (b) 41 min after the start of octylammonium solution flow (*i.e.* 41 min after the first image); the exchange reaction between K^+ and organic ions causes the formation of swelling fronts (height $\approx$ 18 Å); (c–f) 94, 158, 262 and 568 min after the first image: the arrows with labels indicate the different locations of the reaction fronts within the respective interlayers; front '4' is ~100 Å in height. Phlogopite No. 1, scan size 8.8 μm × 8.8 μm.

layers emerging from the same cleavage step. A black solid arrow in Figure 1c indicates a reaction front which emerged from the central cleavage step and propagated undisturbed underneath the layers marked by the right step. It can be seen that the part of the front covered by these additional layers appears more round and less distinct in the AFM images than the parts which were covered by fewer layers (Figure 1c, dashed black arrow). Thus the vertical position of the reacting interlayer can be roughly estimated by the morphological appearance of the fronts in the AFM images. For example, the reacting interlayer 2 (Figure 1c) is lower than the reacting interlayer 1.

Figures 1d–e show a third reaction front emanating from the right cleavage step (Figure 1d, white arrow 3). This third front caught up and merged with the first front (which emanated from the same cleavage step); where merged (Figure 1e, black arrow) bulges were formed (height $\approx$25 nm). From the morphological appearance of the front it followed that the first and the third reactions took place closer to the surface than the second. Therefore, it might be tempting to assume that the ion-exchange rate within interlayers close to the surface is greater than within lower interlayers. However, the distance to the surface is not an exclusive parameter controlling the front propagation rate. Fronts were observed in different layers which had approximately the same propagation rate.

Figure 1f shows the propagation of a fourth swelling front generated by the right cleavage step (white arrow 4). In the upper part of Figure 1f, this front propagated uniformly, but split into two fronts in the lower part (black arrow). The total vertical interlayer expansion at this front was ~100 Å. Additionally, in Figure 1f, three parallel bulges can be seen extending from the cleavage step to the front boundary.

Figure 2 reveals further insights into the ion-exchange reactions at room temperature. Figure 2a shows the initial stage of swelling at a step on phlogopite No. 2. Swelling did not affect the entire step at once, but initiated at a certain position of the step and propagated along the step. The reaction front consisted of two parts, a lower front (height $\approx$10 Å; black arrow) and a higher front (height $\approx$30 Å; white arrow). The propagation of the higher front along the step ceased temporarily (Figure 2b). Eventually, the lower front also stopped to propagate along the step (black arrow in Figure 2c), while the reaction still proceeded inward into the

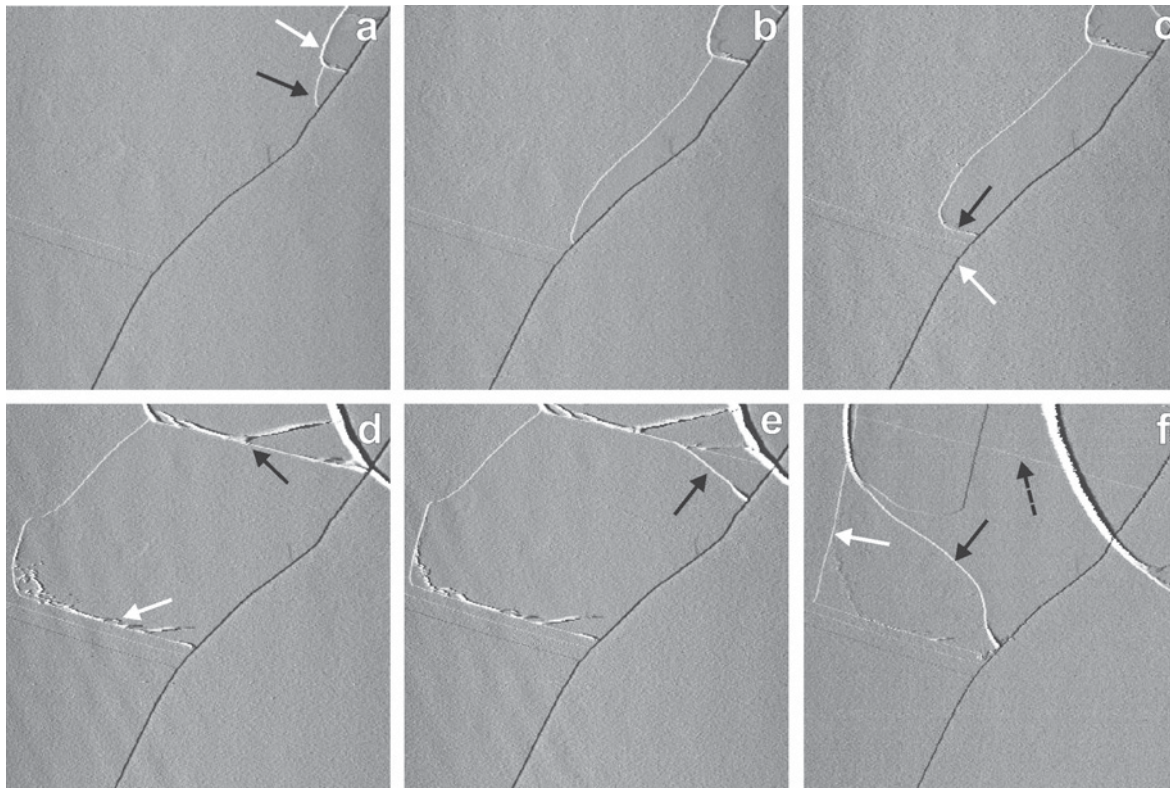

Figure 2. Variation in interlayer reactivity: (a−b) 30 and 65 min after the start of octylammonium solution flow: one front (black arrow, height ~10 Å) propagates along the step, a second front (white arrow, height ≈30 Å) ceased propagation along the step and proceeded exclusively inwards into the interlayer; (c−d) 85 and 1404 min after the first image; the first front also ceased propagation along the step and started to propagate inwards; (e−f) 1509 and 2960 min after the first image, the second front split into two sub-fronts. Phlogopite No. 2, room temperature, scan size 12.5 μm × 12.5 μm.

interlayer. It is worth mentioning that the step in the lower part of the image underwent no alteration for as much as 52 h (Figure 2d). The lower front propagated continuously creating a sharp boundary towards the lower part of the image (Figure 2d, white arrow) until the front movement eventually ceased in Figure 2f (white arrow). Figure 2d (black arrow) shows that the higher front split into a higher (~20 Å, Figure 2e,f, solid black arrow) and a lower (~10 Å, Figure 2f, dashed black arrow) sub-front.

The AFM experiments further revealed that the ion-exchange reaction can be induced by scanning the surface with high loading forces. Figure 3a shows the phlogopite surface after 28 h in solution. The application of high loading forces (~30 nN, black arrows in Figure 3b) triggered new reaction fronts at positions which were unreactive throughout the entire period of scanning with loading forces of ~10 nN.

Octylammonium → K^+ (the reverse ion-exchange reaction)

The *in situ* exchange of the octylammonium solution for the KCl solution triggered a reverse reaction, *i.e.* the front between expanded and pristine areas retreated and the original morphological state was restored. The reverse reaction is shown in Figure 4 which continues Figure 1. The interlayers shrunk in the reverse sequence as they expanded: the later an interlayer expanded, the earlier it shrunk. The shrinking can be explained by a reverse ion-exchange reaction: octylammonium ions left the interlayer, K^+ ions entered.

In Figure 4b, the formation of a small trench (white arrow) within the expanded layer can be seen. While the left front of the trench further retreated, the right front remained stationary. Thus, the progressing reaction generated a completely isolated swollen area containing octylammonium ions (Figure 4c−e). The isolated area remained unchanged for the rest of the experiment (20 h) and only by scanning with high loading forces (~15−20 nN) could minor shape changes be induced. In Figure 4e (white arrow), an island can be seen which remained temporarily connected to the expanded interlayer. Until a complete cut off, the lateral size of the area continued to decrease while the height increased, resulting in the formation of a hillock. A comparison of Figures 1a and 4f shows that apart from the two hillocks the surface is restored to its original morphological state by the reverse ion-exchange reaction.

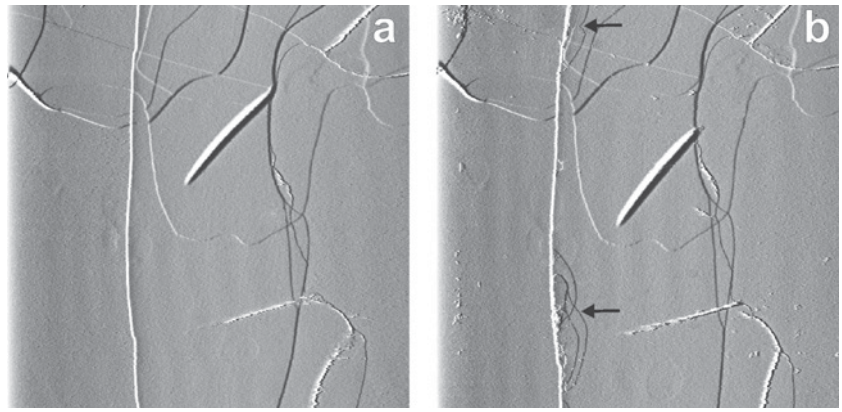

Figure 3. Influence of high loading forces on the ion-exchange reaction: (a) 28 h in octylammonium solution; (b) 35 min later, scanning with high loading forces (~30 nN) triggered further ion-exchange reactions at the same step. Phlogopite No. 2, room temperature, scan size 16.4 μm × 16.4 μm.

Figure 5a shows further structures generated by the reverse ion exchange. In addition to engulfed islands, bulge-shaped surface elevations were observed; the height of the bulges reached up to 50 nm which demonstrates the high elasticity of the silicate layers. The arrow in Figure 5a marks a bulge probably damaged by the scanning tip. Some 54 min later (Figure 5b, slightly scaled up), a complete reorganization of the bulges was observed. One bulge split into smaller separate units, which remained in contact with the islands. The damaged bulge was removed and the engulfed octylammonium islands changed their shape.

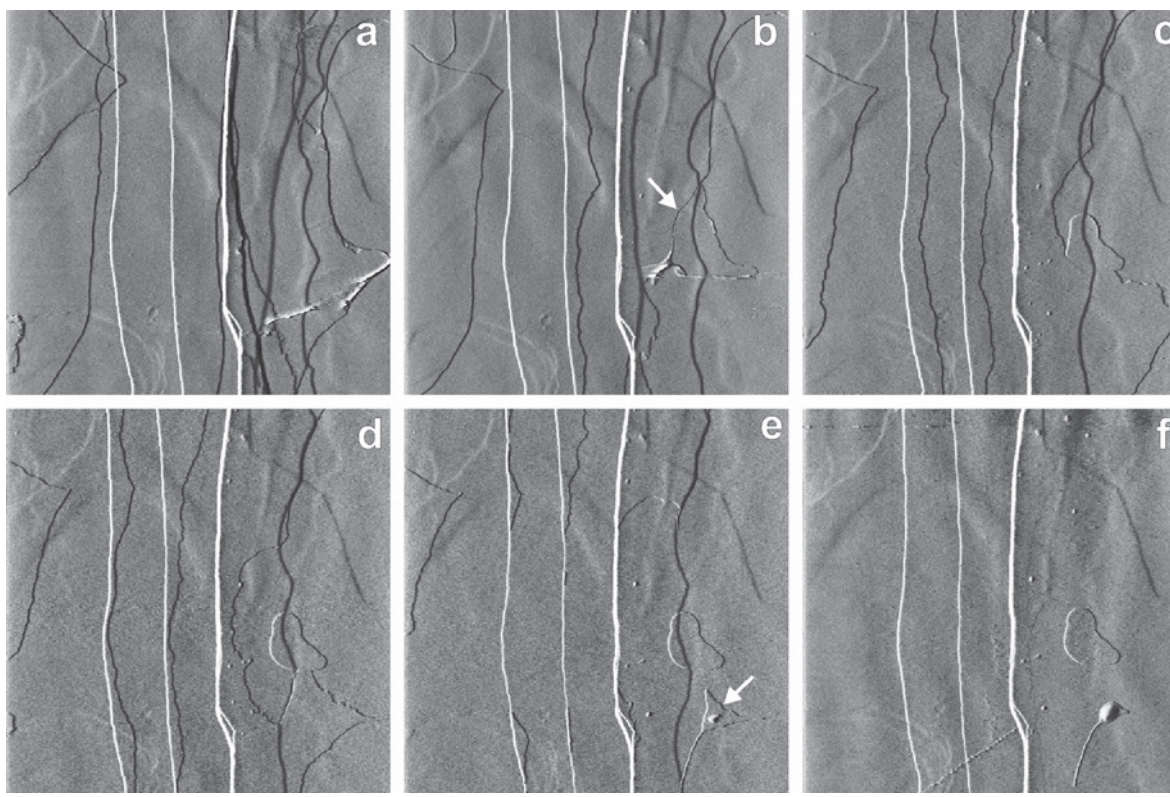

Figure 4. Reverse exchange reaction octylammonium → K^+ (continuation of Figure 1): (a) 97 min after switching to KCl solution flow; the solution exchange causes shrinking of the expanded areas by the retreat of existing fronts exclusively; (b) 30 min later; a trench (white arrow) has been formed within the expanded layer; (c–e) 69, 71 and 85 min after the first image: the formation of an engulfed area can be seen; (f) 203 min after the first image: the originally morphological state was largely restored (c.f. Figure 1a). Phlogopite No. 1, room temperature, scan size 8.8 μm × 8.8 μm.

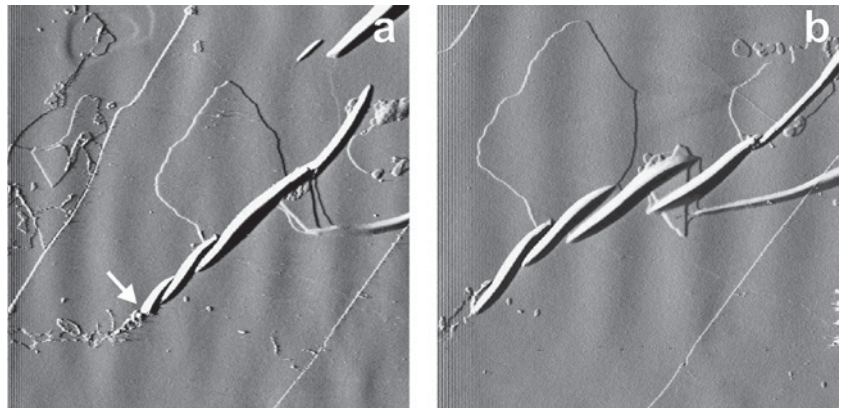

Figure 5. Swelling structures generated by the reverse ion exchange: (a) isolated areas with octylammonium ions and bulges (height up to 50 nm) demonstrate the high elasticity of the silicate layers; scan size 6.5 μm × 6.5 μm; (b) 54 min later: a complete reorganization of the bulges can be observed. Phlogopite No. 1, room temperature, scan size 5 μm × 5 μm.

K^+ → octylammonium (2^{nd} forward reaction)

After the original morphological state of the surface had largely been restored, the KCl solution was re-exchanged for octylammonium. The second octylammonium treatment resulted in a rate of advance of the reaction fronts 10 to 15 times greater within areas which had been subjected to a previous octylammonium treatment. When the fronts entered pristine surface areas, the rate of advance decreased to a value corresponding to the initial octylammonium treatment. Additionally, the second octylammonium treatment caused the bulges generated by the reverse reaction (see Figure 5) to decrease in height – some bulges were even removed completely.

Kinetics of the ion-exchange reactions

As shown above, the movement of the ion-exchange reaction front in phlogopite interlayers was generally not uniform, some fronts even temporarily stopped propagating. Nevertheless, data of the front position as a function of time could be taken at selected fronts which were propagating continuously. Figure 6a depicts the positions of four different reaction fronts progressing from cleavage steps as a function of time. The data were taken in different experiments at 20ºC (RT 1-3) and at 80ºC. The runs RT 1-3 cover the reaction K^+ → octylammonium as well as the reverse reaction octylammonium → K^+. The reverse reaction was started after 290 min in RT 1 (~17 $min^{½}$), 200 min in RT 2 (~14 $min^{½}$), and 630 min (~25 $min^{½}$) in RT 3. Figure 6b shows the rates of the front movement in RT 3. As can be seen, the rate of the forward reaction was much slower than the reverse reaction. At the initial stage the forward rate is ~0.4 nm/s, then drops to 0.1 nm/s, and decreases to ~0.03 nm/s. At ~25 $min^{½}$ the reverse reaction started and the retreat rate rapidly reached ~0.4 nm/s.

From the data in Figure 6 the reaction mechanism can be inferred. In the case of RT 2 and RT 3, the distance traversed by the K^+ → octylammonium front is a linear function of the square root of time that points towards a diffusional mechanism of the reaction. Based on various fronts in several experiments, the diffusion coefficient at room temperature has been estimated to be $1.2 \pm 0.6 \times 10^{-11}$ cm^2/s. The large error range of the diffusion coefficient emphasizes that many fronts show a less perfect relationship between velocity and square root of time than RT 2 and RT 3 (cf. RT 1 and 80ºC) and that the velocities of fronts generated at a given step exhibited some variability. In particular, ~40% of fronts showed a clear diffusional type of movement, another ~40% of fronts showed a more or less constant movement, and ~20% of fronts revealed erratic velocities over the entire experiment.

High-F phlogopite No. 3

In situ AFM experiments on phlogopite crystals with a fluorine concentration of ~6.7 wt.% (see Experimental) showed that the crystals did not react with octylammonium within the timeframe of the experiments; even after 20 h in octylammonium solution, no reaction could be detected on the mineral surfaces. Also, heating the system to 60ºC did not cause any visible alteration.

DISCUSSION

Two important characteristics of the ion-exchange process can be explored in single-layer resolution by the experiments: the value of interlayer swelling and the reaction rate. For an adequate interpretation of the results, the arrangement of the organic ions within the interlayer needs to be considered first. Due to the high layer-charge of phlogopite, alkylammonium ions can form ionic bonds with the silicate layers. For a most effective bonding, the ionic end of the octylammonium ion should be located in the 'hexagonal hole' of the oxygen surface of the layers (Walker, 1967). However, hydration states of the organic ion may influence the

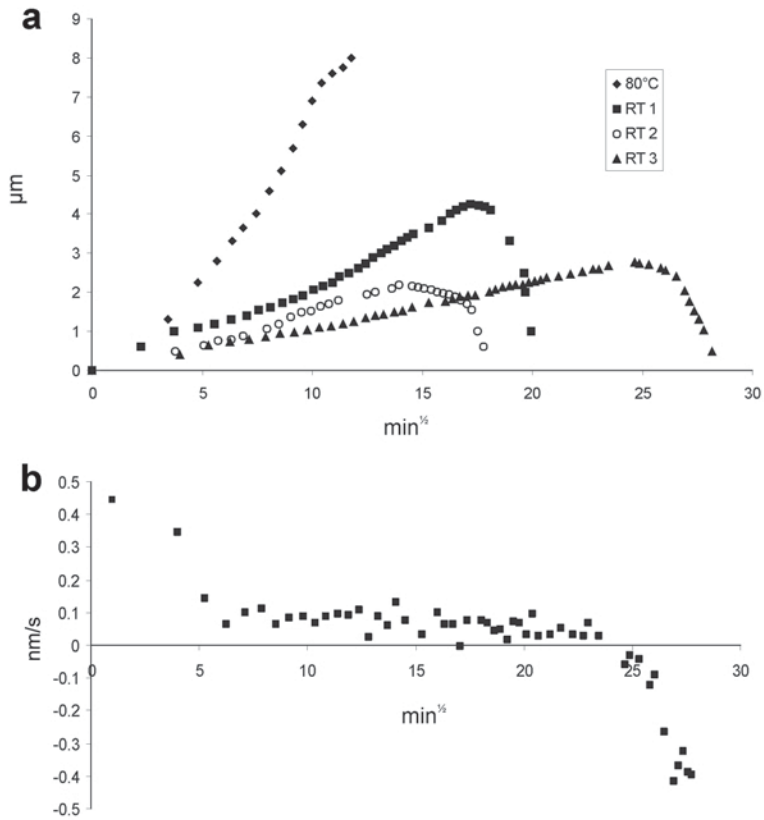

Figure 6. Ion-exchange reaction rates: (a) the positions of four different reaction fronts (three at room temperature, RT 1–RT 3, one at 80ºC) progressing from layer edges are plotted as a function of the square root of time; the data sets RT 1–RT 3 present the data for both K^+ → octylammonium and octylammonium → K^+ reactions; (b) front movement rates of RT3; the rates in the negative range correspond to the reverse reaction.

described arrangement. Walker (1967) reported XRD examinations of the basal spacings of dried and undried alkylammonium-vermiculite suspensions. Upon drying, the author revealed a decrease in the basal spacing of ~5.5 Å for hexylammonium ions (10–13 Å for decylammonium) and suggested that this decrease was caused by a considerable number of water molecules within the interlayers of undried samples. According to our data, the height of reaction fronts was ~18 Å (in rare cases, ~10 Å) at steps consisting of a single phlogopite layer and reached up to ~100 Å at multilayer steps. 10 Å might correspond to a single layer of non-hydrated octylammonium ions oriented almost perpendicular to the silicate layer. The maximum length (trans-trans-modification) of an octylammonium molecule is ~12.5 Å. The most common 18 Å front height can be explained in two ways: (1) a single layer of hydrated octylammonium ions; (2) a double layer of non-hydrated octylammonium ions. In view of the data presented by other authors (*e.g.* Weiss, 1963; Walker, 1967) the single-layer arrangement of hydrated ions seems to be more reasonable, although the existence of 10 Å steps indicates that non-hydrated ions can also occur in single layer arrangements.

Phlogopite layers exhibit different abilities to react with octylammonium. In the case of high-fluorine phlogopite No. 3, no reaction was detected. Low reactivity of high-fluorine micas was also reported by Mackintosh *et al*. (1971). These authors have studied factors influencing the dodecylammonium-exchange reaction in micas with various chemical compositions. High fluorine content has been detected to impede the exchange reaction. The effect has been attributed to the interaction of interlayer K^+ with F^- and OH^- in the octahedral sheet (Bassett, 1960; Rausell-Colom *et al.*, 1964). Potassium ions are supposed to be more strongly bound to the silicate layers, if the octahedral sheet contains F^-, whereas the interaction between K^+ and the protons of structural OH^- groups weakens the bonds.

The experiments with low-F phlogopite No. 1 and 2 showed a considerable variability of the layer reactivity. Even within a single phlogopite sample, the rate of the exchange reaction varies from layer to layer. In total, only 40% of measurements revealed a clear rate *vs*. square root of time relation that points to a diffusion-controlled mechanism of the ion-exchange reaction. The other 60% of measurements gave constant or erratic rate *vs.* time relations. The structural and chemical inhomo-

geneity of natural mica crystals can clearly be regarded as one reason for the observed variability in the reaction kinetics of the interlayers. This inhomogeneity may arise, for example, from a local presence of F^- or Fe as well as variations in the Fe oxidation state, just to name a few possibilities. Also, external disturbances such as increased loading forces (Figure 3) clearly reveal the pronounced sensitivity of the layer reactivity on even small irregularities.

The ion-exchange reaction has been observed to emerge exclusively from layer edges. No reaction emanating from a position within the layer area (e.g. nucleating at point defects) has been detected. The AFM observations further show that the ion-exchange reaction was usually triggered only at certain positions along a layer edge. These positions are located at straight steps rather than at rough or kinked steps. Thus, it can be inferred that the initial stage of the ion-exchange reaction is controlled by chemical characteristics rather than by morphological peculiarities.

Reversing the exchange (*i.e.* octylammonium → K^+) revealed further important details of the alkylammonium−phlogopite reaction. Since octylammonium can be trapped within the interlayers, it follows that octylammonium ions can only be transported within interlayers with increased spacing and can enter and leave this interlayer space only at layer edges but not at the reaction fronts where the silicate layer is considerably strained. Consequently, in contrast to the forward reaction, the reverse reaction cannot emanate from steps because it is self-blocking.

Rausell-Colom *et al*. (1964) reported a diffusion coefficient of ~10^{-10} cm^2/s for the exchange of K^+ by Sr^{2+} in biotite at room temperature in 1 N SrCl solution. As expected from the different size and nature of the ions and molecules used (Sr^{2+}: 2.4 Å; octylammonium: 12.5 Å), the diffusion coefficient obtained in our experiments is lower. It further needs to be taken into account that in the present study the observation of the front movement was limited to the few uppermost layers and to the initial 10 to 15 μm, whereas other authors (Rausell-Colom *et al*., 1964; Walker, 1959) report movements of fronts within the range 0.05−1 mm.

Apart from some areas with trapped octylammonium and some bulges, the surface returned to its original morphological state by the reverse exchange reaction, *i.e*. the silicate layers were linked together by unhydrated K^+ ions. However, the high initial rates of the second octylammonium treatment indicate that in spite of the morphological identity the crystallographic structure had not been restored perfectly. Thus, it can be inferred that the structure of the interlayer undergoes irreversible changes by the reaction K^+ → octylammonium → K^+.

As shown by Rausell-Colom *et al*. (1964), the ion-exchange reaction causes corrugation of silicate layers which can even be detected by optical microscopy. The formation of protuberances and small bulges observed during the first K^+ → octylammonium exchange in the present study (Figure 1e−f) might be considered as an initial stage of the layer folding which has been reported to accompany the alteration (Rausell-Colom *et al*., 1964).

CONCLUSIONS

The application of AFM provides information about the kinetics of ion-exchange reactions *in situ* and with a resolution of single layers. The results show that the exchange of K^+ by octylammonium is emanating from layer edges. The exchange is reversible: from the restored interlayer spacing it follows that K^+ can be reintegrated into the interlayers. However, as indicated by the second forward reaction, irreversible structural changes remain. Also, the reverse reaction (*i.e*. K^+ restoration) usually remains incomplete to some degree; organic ions get trapped within the interlayer. From these results it can be concluded that octylammonium ions exclusively enter and leave the phlogopite interlayers at the layer edges.

The rate of the ion-exchange reaction is far from being uniform. The exchange rates differ substantially between different interlayers within a single crystal and even differ significantly within a single interlayer. Thus it can be concluded that the main factors controlling the exchange reaction rate are inhomogeneities in the chemical and structural integrity of the crystal.

ACKNOWLEDGMENTS

Funding for this project has been provided by the Deutsche Forschungsgemeinschaft (Jo301/2-1) which is gratefully acknowledged. The authors also wish to thank Heinz-Jürgen Bernhardt (Ruhr-Universität Bochum, Germany) for performing the EPM analysis, Hans-Peter Schertl (Ruhr-Universität Bochum, Germany) for providing excellent samples, and Anatoly Aldushin (Russian Academy of Science) for helpful discussion. Furthermore, helpful suggestions of Associate Editor Jim Amonette (Pacific Northwest National Laboratory, Richland, USA), Kevin Rosso (Pacific Northwest National Laboratory, Richland, USA), and two anonymous reviewers are gratefully acknowledged.

REFERENCES

Aldushin, K., Jordan, G. and Schmahl, W.W. (2006) Basal plane reactivity of phyllosilicates studied *in situ* by hydrothermal atomic force microscopy (HAFM). *Geochimica et Cosmochimica Acta*, **70**, 4380−4391.

Barshad, I. and Kishk, F.M. (1968) Oxidation of ferrous iron in vermiculite and biotite alters fixation and replaceability of potassium. *Science*, **162**, 1401−1402.

Bassett, W.A. (1960) Role of hydroxyl orientation in mica alteration. *Geological Society of America Bulletin*, **71**, 449−455.

Ferrow, E.A., Kalinowski, B.E., Veblen, D.R. and Schweda, P. (1999) Alteration products of experimentally weathered biotite studied by high-resolution TEM and Mössbauer spectroscopy. *European Journal of Mineralogy*, **11**,

999–1010.

Ghabru, S.K., Mermut, A.R. and St. Arnaud, R.J. (1989) Layer-charge and cation-exchange characteristics of vermiculite (weathered biotite) isolated from a Gray Luvisol in north-eastern Saskatchewan. *Clays and Clay Minerals*, **37**, 164–172.

Higgins, S.R., Eggleston, C.M., Knauss, K.G. and Boro, C.O. (1998) A hydrothermal atomic force microscope for imaging in aqueous solution up to 150ºC. *Review of Scientific Instruments*, **69**, 2994–2998.

Jordan, G., Higgins, S.R., Eggleston, C.M., Knauss, K.G. and Schmahl, W.W. (2001) Dissolution kinetics of magnesite in acidic aqueous solution, a hydrothermal atomic force microscopy (HAFM) study: Step orientation and kink dynamics. *Geochimica et Cosmochimica Acta*, **65**, 4257–4266.

Kodama, H. and Ross, G.J. (1973) Structural changes accompanying potassium exchange in a clay-size muscovite. Pp. 481–492 in: *Proceedings of the International Clay Conference, Madrid 1972*, (J.M. Serratosa, editor). Div. Ciencias C.S.I.C., Madrid.

Lagaly, G. (1981) Characterization of clays by organic compounds. *Clay Minerals*, **16**, 1–21.

Lagaly, G. (1991) Erkennung und Identifizierung von Tonmineralen mit organischen Stoffen. Pp. 86–130 in: *Identifizierung und Charakterisierung von Tonmineralen* (H. Tributh und G. Lagaly, Hrsg.). Berichte der Deutschen Ton- und Tonmineralgruppe, DTTG, Gießen, Germany.

Lagaly, G. and Weiss, A. (1969) Determination of the layer charge in mica-type layer silicates. In: *Proceedings of the International Clay Conference, Tokyo, 1969*, Vol. 1 (L. Heller, editor). Israel University Press, Jerusalem.

Laird, D.A., Scott, A.D. and Fenton, T.E. (1987) Interpretation of alkylammonium characterization of soil clays. *Soil Science Society of America Journal*, **51**, 1659–1663.

Mackintosh, E.E., Lewis, D.G. and Greenland, D.J. (1971) Dodecylammonium-mica complexes – I. Factors affecting the exchange reactions. *Clays and Clay Minerals*, **19**, 209–218.

Marcks, C., Wachsmuth, H. and von Reichenbach, H.G. (1989) Preparation of vermiculites for HRTEM. *Clay Minerals*, **24**, 23–32.

Mermut, A.R. and Lagaly, G. (2001) Baseline studies of the Clay Minerals Society source clays: Layer-charge determination and characteristics of those minerals containing 2:1 layers. *Clays and Clay Minerals*, **49**, 393–397.

Newman, A.C.D. (1970) The synergetic effect of hydrogen ions on the cation exchange of potassium in micas. *Clay Minerals*, **8**, 361–373.

Rausell-Colom, J.A., Sweatman, T.R., Wells, C.B. and Norrish, K. (1964) Studies in the artificial weathering of mica. Pp. 40–72 in: *Experimental Pedology* (E.G. Hallsworth and D.V. Crawford, editors), Butterworth, London.

Ruehlicke, G. and Kohler, E.E. (1981) A simplified procedure for determining layer charge by the n-alkylammonium method. *Clay Minerals*, **16**, 305–307.

Vali, H., Hesse, R. and Kodama, H. (1992) Arrangement of n-alkylammonium ions in phlogopite and vermiculite: an XRD and TEM study. *Clays and Clay Minerals*, **40**, 240–245.

Walker, G.F. (1959) Diffusion of exchangeable cations in vermiculite. *Nature*, **184**, 1392–1393.

Walker, G.F. (1967) Interactions of n-alkylammonium ions with mica-type layer lattices. *Clay Minerals*, **7**, 129–143.

Weiss, A. (1963) Mica-type layer silicates with alkylammonium ions. *Clay Minerals*, **10**, 191–224.

(*Received 26 October 2006; revised 20 March 2007; Ms. 1231; A.E. James E. Amonette*)